

---

## Sub-millinewton tribometer to measure friction and stiffness of flat-on-flat contacts

Sander Paalvast<sup>1</sup>, Maurice Teuwen<sup>1</sup>, Huub Janssen<sup>1</sup>

<sup>1</sup>JPE, Maastricht-Airport, The Netherlands

[sander.paalvast@jpe.nl](mailto:sander.paalvast@jpe.nl)

---

### Abstract

This paper describes the development and qualification of a tribometer to measure the dynamic and static coefficients of friction and contact stiffness of flat-on-flat mechanical contacts in both ambient and vacuum. The tribometer is used to validate and further develop models of these types of contacts in state-of-the-art equipment working with thin substrates. With these models the errors introduced by the contact deformation under mechanical and thermal loads can be predicted for design optimization or for correction by feedforward control. The novelty of the tribometer is in its ability to measure both lateral and normal contact stiffness of stiff flat-on-flat contacts, in the order of  $10^6$  to  $10^7$  newton per metre, under normal loads as low as 5 mN. To build such an instrument, a range of precision engineering and mechatronic challenges had to be solved from reproducible sample mounting to tuning feedback controllers to be robust against the changes in dynamic response when the contact stiffness increases by orders of magnitude. Besides discussing the design, the paper also presents the results of the system level qualification which was done by measuring the well-known stiffness, in six degrees of freedom, of a special stiffness qualification sample. These results show that the tribometer can uniformly apply a normal load of 3 mN per contact with 0.6 mN precision, measure friction forces as low as 0.3 mN with a precision of 0.1 mN ( $3\sigma$ ), and measure lateral and normal displacements / deformations with 0.05 and 0.06 nm resolution, respectively.

Keywords: Precision engineering, Mechatronics, Tribology

---

### 1. Introduction

Thin substrates processed in semiconductor manufacturing equipment must be positioned reproducibly to align the many layers that make up an integrated circuit. With shrinking feature size, the positioning requirements become so stringent that the sub-nanometre deformations in the many flat-on-flat contacts between the substrate and its handler must be compensated for. Lacking a direct measurement, or feedback signal, models are employed to predict the required compensation. To develop and validate these models one cannot rely on just the data generated by classic pin-on-disc experiments because the presliding regime is dominated by the adhesive forces owing to asperity contacts [1] which depend on the manufacturing process and the use case. Therefore, a customer commissioned the design and realization of a tribometer for measuring the properties of exactly replicated contacts, in terms of geometry and conditions, as found in their products. They required the instrument to measure lateral and normal contact stiffness in the range of  $10^4$  to  $2 \cdot 10^6$  N/m at normal loads from 3 mN to 10 mN with an accuracy of thirty percent, or better, and  $10^4$  to  $10^7$  N/m above 10 mN up to 2 N with ten percent accuracy. Furthermore, it must be able to measure at ambient conditions, in dry air, and in high vacuum ( $10^{-5}$  mbar).

Following a build, test, learn approach, to deal with the uncertainties in the requirements and design, the first tribometer was put into operation early 2015 and saw several minor upgrades in hardware and software. The design and some of the mechatronic challenges encountered during its development and realization have been discussed in a previous paper, Ref. [2]. Once the boundaries of fine-tuning were reached and many uncertainties clarified, a major upgrade was planned to replace the displacement sensors which were the bottleneck

in measuring contact stiffness at low normal loads and low Coefficients of Friction (CoF). For example, when the stiffness is  $10^6$  N/m at 3 mN, the displacement corresponding to the maximal lateral force of 0.3 mN (minimal CoF of 0.1) is only 0.3 nm for the linear (stiffness) part of the pre-sliding curve. This leads to a desired resolution for the displacement and force metrology of 30 pm and 30  $\mu$ N, respectively.

In the next section the concept and design of the tribometer will be discussed focussing on the upgraded parts. The following section describes the feedback loops to control the normal load per contact and the position of lateral stage. Section four presents the qualification highlights and the final section summarizes the conclusion and outlook.

### 2. Design

The already challenging requirements are further complicated by the demand to exactly replicate contact geometry and conditions. Independent of the size of the area and the material of the samples the instruments must apply a uniform pressure over the contact areas. Having samples with three contact areas, to create an inherently stable interface (exact kinematic constraint), helps to achieve this. The next steps were to design the subsystem and a procedure to align the top samples with respect to the bottom sample in the out-of-plane Degrees of Freedom (DoF) z, Rx, Ry.

#### 2.1. Concept

Figure 1 shows the concept of the tribometer which was discussed before in Ref. [2]. The contact sample is mounted on a stage which can move in two directions. It is actuated by three piezo actuators and the resulting forces are measured by three force cells. Two actuators and sensors would have sufficed, but

the symmetric design improves stability by creating a thermal centre at the heart of the sample.

The counter surface sample is mounted in the so-called top sample interface which can be moved in three out-of-plane degrees of freedom using three piezo actuators (same design as the lateral actuators) for sample alignment and contacting. Once in contact, the piezo displacement is mostly absorbed in the normal force cells, behind the actuators, because their stiffness of about  $10^5$  N/m is typically lower than the contact stiffness. This effectively turns the position actuation into force actuation with the advantage of low power consumption and thus low thermal load compared to electromagnetic force actuation. Flexure mechanism guide constrain and the samples to guarantee reproducibility of the (parasitic) forces and motions.

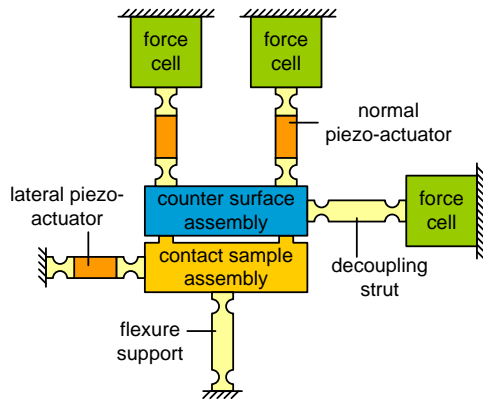


**Figure 1.** Concept of the flat-on-flat tribometer with piezo actuators to move the contact sample, supported by flexures, in lateral direction and to apply a uniform normal load to three contacts.

## 2.2. Displacement and force metrology

Although the displacement metrology is relevant for friction measurements, to determine the transition point from static to dynamic friction and the sliding velocity, the most demanding requirements come from the contact stiffness measurements. At normal loads in the order of (tens of) millinewton the deformations are typically sub-nanometre because the lateral force is limited by the typically low (0.1) to modest (0.3) coefficient of friction of the samples. While in normal direction more, and thus smaller, displacement increments are needed to characterize non-linearity of the force-displacement curve. To meet these requirements, the tribometer is equipped with six Zygo® ZPS absolute position sensors with 10 pm resolution and a measurement range of hundreds of micrometres [3].

At higher normal loads (0.1 ~ 2 N), when the stiffness approaches  $10^7$  N/m, accurate displacement measurements is achieved by separating the metrology, shown in Figure 2, and force frames to keep deformations of the force frame outside the critical measurement loop and by using materials with relatively high stiffness, whenever possible, inside the loop, e.g. tungsten-carbide sample holders.

Custom force cells were developed because commercially available force sensors could not meet the required combination of over 2 N range and 30  $\mu$ N resolution or could not measure a constant force (normal load). The working principle of the force cells is to measure the deformation of titanium monolithic flexure mechanism, for reproducibility and stability, and from that calculating the applied force. With the upgrade the force cells got new internal sensors, also ZPS absolute position sensors, for higher force resolution and absolute instead of relative force measurements. Furthermore, dampers were integrated in the force cells to dampen the rigid body modes of the assembly holding the counter surface sample as discussed in

Section 2.4. The stiffness of each individual force cell ( $1.1\sim 1.2\cdot 10^5$  N/m), was calibrated using calibrated weights before integration into the instrument.

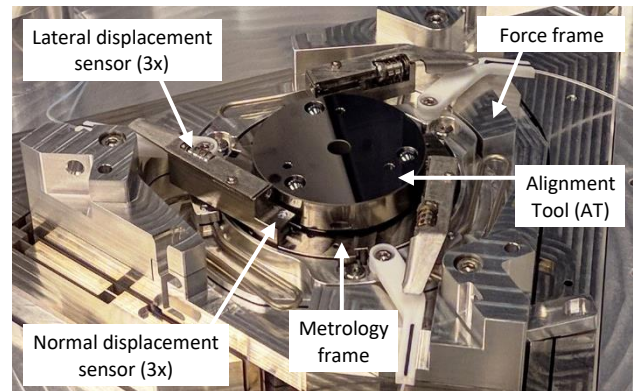


**Figure 2.** Photograph of the lateral stage showing the separated metrology frame, with displacement sensors, and force frame.

## 2.3. Sample interface

Both samples are glued to their (specific) tungsten-carbide sample holder to keep the local angles of the contacting surfaces small, typically below 20  $\mu$ rad, and thus replicate the flatness of the thin substrate in the customers application. To maintain this flatness when mounting the samples and achieve high stiffness between the metrology frame and the sample, an innovative sample interface was developed together with the project partner responsible for the sample holders and the sample preparation procedures and tooling.

The concept is shown in Figure 3 and is based on the interface design from Ref. [4]. The holder is clamped between the force frame (fixed world) and metrology frame via ball/V-groove interfaces. Three of the interface sets constrain the DoFs of the frames exactly. 30 N is applied per ball/V-groove by a preload spring with a relatively low stiffness of  $10^3$  N/m to create a stiff connection insensitive to variations, e.g. of the lateral load on the sample. Because the holder is under purely compressive load the local angles of the sample remain unchanged. The soft spring first fully locates the sample holder before the preload is applied, achieving sub-micrometre positioning reproducibility.

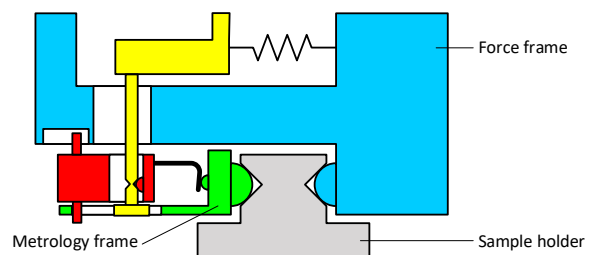


**Figure 3.** Concept of the interface for sample mounting

## 2.4. Vibration isolation and damping

To isolate floor vibrations the tribometer is placed on a vibration isolation table with commercial air-mounts, schematically depicted in Figure 4. The connections are made through the bottom of the environment chamber via steel, low stiffness bellows to stop the vibrations from entering through this path. Vibrations from the vacuum turbo pump are eliminated by using a pump with electro-magnetic bearings and by bolting its independent frame stiffly to the floor.

On top of the measures above, passive dampers were integrated in the force cells to attenuate the rigid body modes of the top actuation and metrology assembly by approximately twenty times in the frequency range of 40 to 60 Hz. These so-

called robust mass dampers consist of a stainless steel moving mass of about 100 g and (vacuum compatible) rubber leaf springs. In normal direction a coil spring applies the weight compensation force to avoid creep issues.

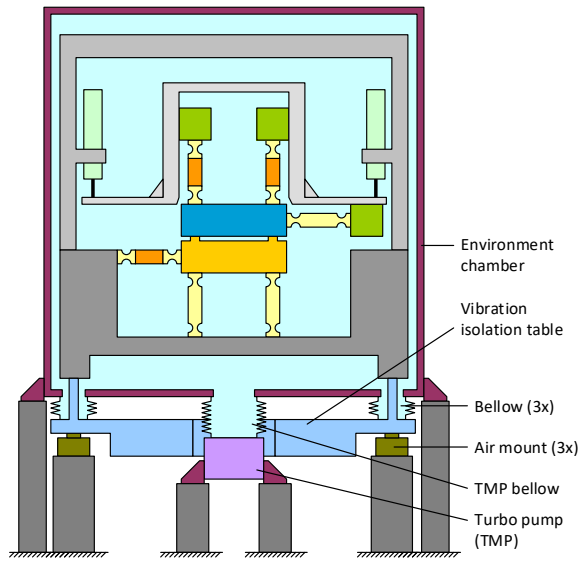


**Figure 4.** Schematic depiction of the vibration isolation through the bottom of the environment chamber on air mounts.

### 3. Operating procedures and control

Before the samples can be brought into contact their contact planes must be aligned. This is done by slowly scanning for contact with the normal piezo actuators and normal force cells to detect the (steep) increase in stiffness. The procedure is already described in detail in Ref. [2]. Since then it has been fine-tuned to lower the contacting forces ( $< 5$  mN) and software compensation has been applied to reduce the normal load error caused by parasitic stiffness of the decoupling struts of the lateral force cells (Figure 1) to less than 0.1 mN.

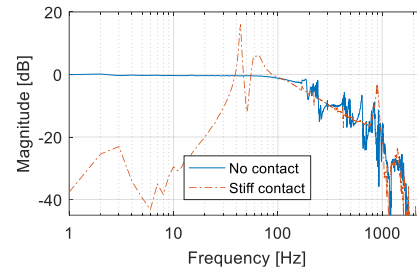
Once the samples are aligned, they are brought into contact using a low bandwidth force controller to keep the force per contact below 3 mN. Then the software switches to the normal load controller described in the next sub-section and increases the load or moves the lateral stage, depending on the type of experiment, following a user defined trajectory. Sub-section 3.2 discusses the feedback controller of the lateral stage position which cancels the drift typical for piezo actuators.

#### 3.1. Normal load control

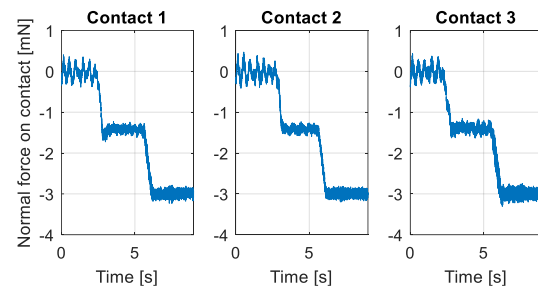
A feedback loop with the normal piezo actuators and normal force cells precisely controls the applied forces, corrected for sample geometry, in the presence of disturbances such as a drift, vibration, and varying lateral loads during the experiments. Besides normal load precision, robustness was an important objective for tuning this control loop because the contact stiffness can vary by several orders of magnitude. Figure 5 demonstrates the resulting change in dynamic response of a single contact from zero (no contact) to 1 N normal load.

Figure 6 shows the force signals during the contacting procedure. Initially, the low bandwidth contacting controller is active. Its integrator gain determines the approach / impact velocity and it has been tuned to keep the velocity below  $1 \mu\text{m/s}$  corresponding to an impact force below 3 mN. When all three forces are below the threshold of -1.2 mN the contacting procedure switches to a normal load controller with a higher bandwidth (15 vs 4 Hz), i.e. higher disturbance rejection, and

lowers the normal force to -3 mN or any value down to -2 N requested by the operator (decreasing the force corresponds to increasing the compressive load).



**Figure 5.** Frequency response of a single contact from setpoint to measured force without contact and at 1 N normal load.



**Figure 6.** Normal forces on the three contacts when making contact. Contact is established between  $t = 2.5$ -3 [s] and the switch from contacting to the normal load controller occurs around  $t = 5$  [s].

#### 3.2. Lateral position control

Small deviations of the relative lateral position of the samples can lead to a large shift of the measurement point on the presliding curve because the gross-sliding regime can start already after a few nanometres' displacement, depending on the coefficient of friction and the normal load.

The issue is observed in the left part of Figure 7 showing 10 back and forth movements with 10 nm displacement without enabling the feedback controller (samples not in contact). The dominant disturbance source is the drift of the piezo actuator at sub-Hertz frequencies where their amplifiers transition from charge to voltage feedback control. A low bandwidth PID feedback controller is enough to suppress this drift and by controlling the stage position, instead of the relative displacement, the control loop is insensitive to the changes of the transfer function due to sample to sample variations and the (non-linear) transition from presliding to gross-sliding regime. The right part of Figure 7 shows that the drift is reduced over two orders of magnitude from 4.4 nm/min to 0.037 nm/min by enabling the controller.

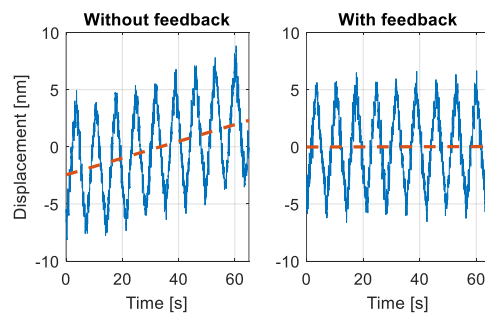


**Figure 7.** Ten back and forth movements without (left) and with (right) feedback position control. Dashed lines show the drift (1<sup>st</sup> order fit).

## 4. Qualification

Acceptance tests were conducted at the customers site to verify the performance of the tribometer from alignment accuracy, to maximal contacting force, achievable normal load range, and environment control. Two highlights will be presented in this section, first the measured displacement and force noise levels and second the qualification of the stiffness measurement accuracy and reproducibility.

### 4.1. Displacement and force noise

To characterize the displacement and force noise, critical for the measurement accuracy and precision at low loads and high contact stiffness, two separate tests were conducted.

The force noise was measured without bringing the samples in contact when the acceleration forces acting on the top assembly / sample interface, generated by vibrations, pass only through the force cells. These are dominating the cumulative Power Spectral Density (PSD), plotted in Figure 8, especially in the region from 1 Hz to 6 Hz due to the rigid body modes of the vibration isolation table. When in contact, these vibration induced forces pass mostly through the (stiffer) contacts and then the precision of the applied forces is equal to the measured  $3\sigma$  noise levels of 0.1 mN and 0.06 mN in lateral direction and 0.5 mN in normal direction for a measurement bandwidth of 24 Hz.

For the displacement noise measurement, the displacements due to frame / floor vibrations were minimized by measuring with two special samples, made completely of tungsten carbide, brought into contact with 2 N normal load to accomplish high contact stiffness (sample 'AT' in Figure 5). The resulting cumulative PSD is plotted in Figure 9 and shows that the  $3\sigma$  noise level of the tribometer is 0.05 nm in the lateral direction and below 0.06 nm in normal direction for a measurement bandwidth of 24 Hz. As for the forces, the rigid body modes of the vibration isolation table dominate the displacement noise (1-6 Hz).

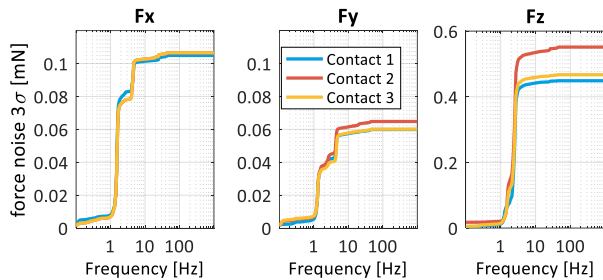


**Figure 8.** Cumulative PSD of the lateral & normal contact force signals (samples not in contact). Noise levels ( $3\sigma$ ) are 0.1 mN, 0.06 mN, and 0.5 mN for Fx, Fy, and Fz, respectively.

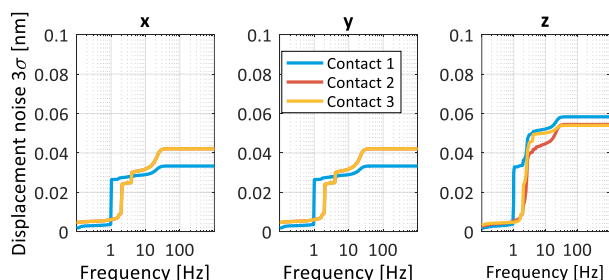


**Figure 9.** Cumulative PSD of the lateral & normal contact displacement / deformation signals (contact stiffness  $> 10^7$  N/m). Noise levels ( $3\sigma$ ) are below 0.05 nm in lateral and below 0.06 nm in normal direction.

### 4.2. Stiffness measurement accuracy & reproducibility

Besides through the qualification of the displacement and force sub-systems, the stiffness measurement accuracy and reproducibility were qualified by measuring the stiffness of a special qualification sample. The sample was designed to have a reproducible and constant 6DoF stiffness corresponding approximately to a sample with three times  $10^6$  N/m contact stiffness in both lateral and normal direction.

The measured stiffness at various normal loads is plotted in Figure 10 together with dashed lines indicating the required accuracy and reproducibility, and the solid line indicates the nominal stiffness (from analysis/FEM). The results show that the measurement accuracy and reproducibility are within the requirement for both lateral directions and the normal direction ( $\leq 30\%$  below and  $\leq 10\%$  above 10 mN load).

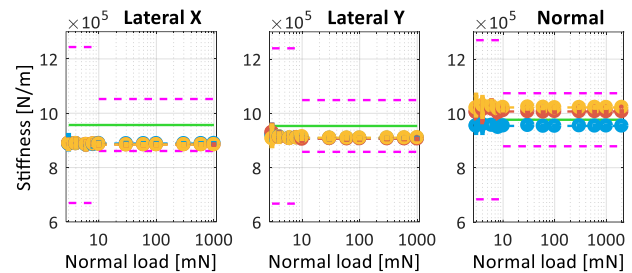


**Figure 10.** Measured stiffness of a special qualification is sample in lateral (X & Y) and normal direction. Dashed lines indicate the requirement and the solid line the nominal stiffness (FEM).

## 5. Conclusion and outlook

A tribometer to measure the coefficients of friction and the contact stiffness and flat-on-flat contacts in ambient air, in dry air, and in vacuum has been developed, realized, and qualified. Qualification results show that it can uniformly apply a normal load of 3 mN per contact with 0.6 mN precision, measure friction forces as low as 0.3 mN with a precision of 0.1 mN ( $3\sigma$ ), and measure lateral and normal displacements / deformations with 0.05 and 0.06 nm resolution, respectively. This could be improved in the future by installing a (active) vibration isolation table with isolation frequency below 1 Hz where the floor vibration spectrum is lower.

The reproducible and constant  $10^6$  N/m stiffness of a special qualification sample was measured well within 30 % accuracy from 3 mN normal load and 10 % for loads above 10 mN. Analysis of the qualification results is ongoing to determine whether these accuracies are achieved over the complete stiffness range from  $10^4$  N/m to  $10^7$  N/m.

### Acknowledgements

The authors gratefully acknowledge the input and collaboration of the customer's tribology team, Entechna Engineering (samples preparation and tooling, stiffness Q-sample, sample to tribometer interface), NTS Development & Engineering (software development), Zygo® Corporation, and our colleagues at JPE.

### References

- [1] Al-Bendar F and Swevers J 2008 Characterization of friction force dynamics *IEEE Control Systems Magazine* **28-6** 64-81
- [2] Paalvast SL *et al.* 2016 Mechatronics of a sub-milliNewton tribometer *Proc. Conf. on Prec. Mechatronics, St Michielsgestel, NL*
- [3] Zygo® Corporation 2016 ZPS™ System specifications SS-0116 05/16
- [4] Werner C 2010 A 3D translation stage for metrological AFM *Doctoral Thesis* 30-32